Appendix

THE JOURNAL OF PHYSICAL CHEMISTRY C

Article

pubs.acs.org/JPCC

Highly Sensitive and Selective Gas Detection Based on Silicene

Jariyanee Prasongkit,*[,†,‡] Rodrigo G. Amorim,[¶,⊥] Sudip Chakraborty,[¶] Rajeev Ahuja,[¶,§] Ralph H. Scheicher,[¶] and Vittaya Amornkitbamrung[∥,‡]

[†]Division of Physics, Faculty of Science, Nakhon Phanom University, Nakhon Phanom, 48000, Thailand

[‡]Nanotec-KKU Center of Excellence on Advanced Nanomaterials for Energy Production and Storage, Khon Kaen, 40002, Thailand

[¶]Division of Materials Theory, Department of Physics and Astronomy, Uppsala University, Box 516, SE-751 20 Uppsala, Sweden

[§]Applied Materials Physics, Department of Materials Science and Engineering, Royal Institute of Technology (KTH), SE-100 44 Stockholm, Sweden

[∥]Integrated Nanotechnology Research Center, Department of Physics, Faculty of Science, Khon Kaen University, Khon Kaen, 40002, Thailand

Supporting Information

ABSTRACT: Recent advances in the fabrication of silicene devices have raised exciting prospects for practical applications such as gas sensing. We investigated the gas detection performance of silicene nanosensors for four different gases (NO, NO_2, NH_3, and CO) in terms of sensitivity and selectivity, employing density functional theory and nonequilibrium Green's function method. The structural configurations, adsorption sites, binding energies and charge transfer of all studied gas molecules on silicene nanosensors are systematically discussed in this work. Our results indicate that pristine silicene exhibits strong sensitivity for NO and NO_2, while it appears incapable of sensing CO and NH_3. In an attempt to overcome sensitivity limitations due to weak van der Waals interaction of those latter gas molecules on the device, we doped pristine silicene with either B or N atoms, leading to enhanced binding energy as well as charge transfer, and subsequently a significant improvement of sensitivity. A distinction between the four studied gases based on the silicene devices appears possible, and thus these promise to be next-generation nanosensors for highly sensitive and selective gas detection.

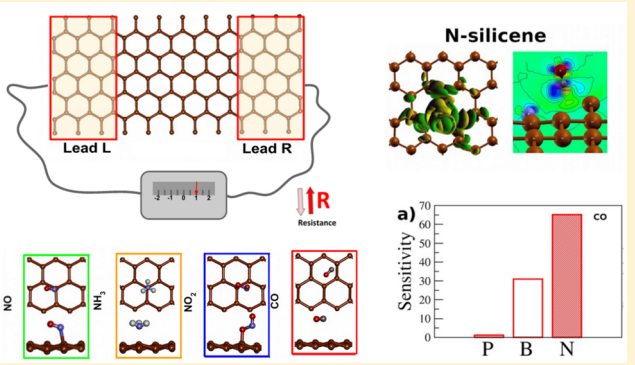

INTRODUCTION

Two-dimensional nanostructure materials have taken the front row in innovative applications in the past decade after the successful experimental exfoliation of graphene. Gas sensors based on graphene have attracted much attention since graphene has excellent sensitivity to detect various gas molecules, large sensing area per unit volume, low electronic temperature noise, fast response time, and high chemical stability.[1,2] The potential use of graphene for gas detection has been intensively investigated both experimentally[3−5] and theoretically.[6−8] However, growth of graphene over large surface areas is constrained. This motivated the search for other materials with similar favorable properties. In turn, this has led to the discovery of silicene as a silicon counterpart. The good properties with versatile silicon based nanotechnology gives the edge to silicene rather than graphene. This serves as the motivation of our work to theoretically explore the applicability of silicene for gas sensing.

The massless Dirac Fermions are the main reasons behind the ultrahigh carrier mobility for both the honeycomb structures of silicene and graphene.[9,10] Geometrically, the hexagonal structure of silicene has a larger size due to the larger ionic radius of Si atoms,[11] but they have similar electronic structures. One important demarcation between the two structures is a buckled formation in silicene. This is due to sp^3 and sp^2 hybridization[12] rather than only sp^2 hybridization. This feature leads to a few prominent differences in the properties of silicene and graphene. Band gap tuning with an external electric field[13,14] and with the binding adsorbates[15−17] can be seen more profoundly in silicene than in graphene.[18,19] Although free-standing silicene has not been achieved so far, recent progress shows that it can be synthesized experimentally by depositing silicon on different surfaces such as silver,[20,21] gold,[22] zirconium diboride,[23] and iridium.[24]

To date, a wide range of potential applications of silicene have been proposed in various field such as spintronics,[25,26] FETs,[27−30] hydrogen storage,[31,32] and sensing devices.[33,34] Nevertheless, using silicene as gas sensor has not been given the

Received: April 16, 2015
Revised: June 25, 2015

DOI: 10.1021/acs.jpcc.5b03635
J. Phys. Chem. C XXXX, XXX, XXX−XXX

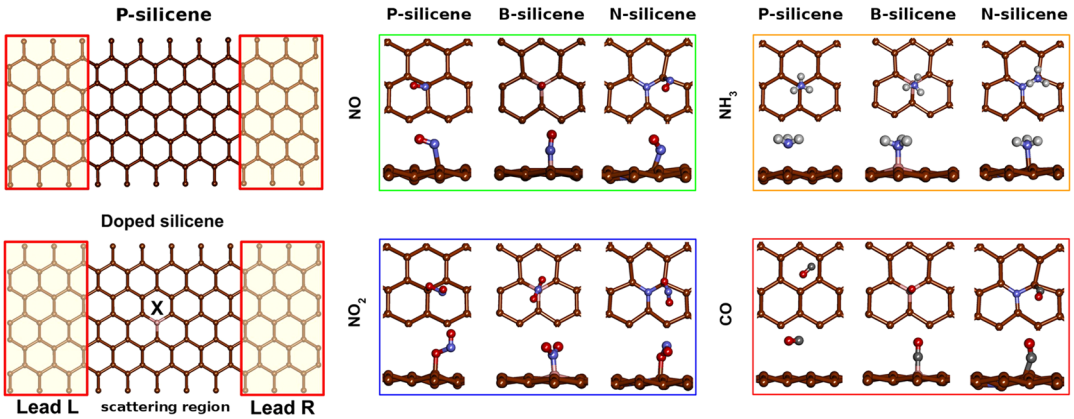

Figure 1. Device setup is shown in the left panel for pristine (upper) and doped silicene (lower) where X marks the site for B and N doping. The central and right panels show the most stable configurations for the four gas species NO, NH_3, NO_2, and CO when adsorbed on either pristine, B-doped or N-doped silicene.

attention it deserves. Two theoretical investigations based on density functional theory (DFT) were done to explore potential application of silicene as a molecular sensor for gas molecules.[35,36] They revealed changes in the electronic structures of silicene with adsorbed gas. The prime parameters to characterize the sensor performance of a gas sensor are sensitivity, selectivity, response time and recovery time. They should be addressed simultaneously to meet real application requirements of silicene based sensing systems.

The purpose of our study was therefore 2-fold. First, we used the state-of-the-art first-principle methods to study the electronic and transport properties to evaluate the gas discrimination of silicene in terms of sensitivity and selectivity. Second, we demonstrate the possibility to improve gas sensing performance of silicene through doping this material with B and N atoms.

In this work, we investigated the electronic and transport properties of gas molecules adsorbed onto pristine (P) and B/N-doped silicene by employing a robust combination of nonequilibrium Green's function (NEGF) techniques and DFT. Four representative gas species—NO_2, NO, NH_3, and CO molecules, which are of main interest for environmental safety and medical purposes, were shown to be detectable by silicene based sensor devices. The sensitivity and selectivity of the devices to the presence of those gas molecules were evaluated from the changes in their electronic transport properties. Our results indicate that doping impurity atoms into silicene can enhance the interaction between the gas molecules and doped devices. This enabled an immense improvement in the performance of this type of sensor.

■ COMPUTATIONAL METHODS

The geometrical structures of four different molecular gases (NO, NO_2, NH_3, and CO) adsorbed on pristine silicene and doped-silicene nanodevices were relaxed by using DFT[37,38] as implemented in the SIESTA package.[39] To describe the weak dispersive interactions, we employed a van der Waals correction[40,41] to the generalized gradient approximation of Perdew, Burke, and Ernzerhof (PBE-GGA)[42] for the exchange-correlation functional in DFT.

A description of van der Waals (vdW) were performed using vdW-DF, as proposed by Dion et al.[40] In this methodology, the exchange-correlation energy is written as

$$E_{xc} = E_x^{GGA} + E_c^{LDA} + E_c^{nl} \quad (1)$$

where the exchange energy E_x^{GGA} uses the GGA functional, and E_c^{LDA} is the local density approximation (LDA) to correlation energy. The nonlocal correlation-energy part, E_c^{nl}, is defined to include the longest-ranged or most nonlocal energy term which is zero for systems with constant density.

For the ionic relaxation 6 × 1 × 4 *k*-points and for the electronic transport 24 × 1 × 1 *k*-points were used. Furthermore, double-ζ polarized basis sets (DZP) and norm-conserving pseudopotentials[43] were used. The conjugate gradient (CG) method was applied to obtain equilibrium structures with residual forces on atoms below 0.01 eV/Å. We also employed VASP[44] code, using the same parameters as in of SIESTA for the relaxation and binding energy calculations with a 400 eV cutoff energy for the plane wave basis and a force tolerance of 0.01 eV/Å. Silicene has a buckled hexagonal lattice, consisting of 2 Si atoms per unit cell. For transport calculation, each simulated system consisted of 20.57 Å × 15 Å × 43.54 Å silicene supercell with 132 Si atoms. We use the periodic boundary condition (PBC) along the *x*-direction and the *z*-direction and considerably large supercell to avoid the interaction occurring between mirror images. The neighboring silicene in the *y*-direction was separated by 15 Å of vacuum. See Supporting Information for additional details on supercell construction.

The transport properties were then investigated with the TranSiesta code,[45] combining the NEGF method and DFT. This was done to perform electronic transport calculations in order to visualize the degree of capability of pristine silicene and doped-silicene nanodevices as an electric nanosensors to distinguish four different molecular gases (NO, NO_2, NH_3, and CO). The basis sets and the real-space grid employed in the transport calculations are identical to those described above for the geometrical optimization part. The system was divided into three parts: two leads (left and right) and a scattering region in between them. The left panel of Figure 1 shows upper (pristine) and lower panel (doped) hexagonal 2D silicene that was used as a molecular gas sensor. The red shaded rectangles represent the electrodes or leads (left/right) and the region in between was the scattering region. Nitrogen (N) and boron (B) are the two substituted atoms used to functionalize silicene.

Defining the boundary as a region, where the charge density matches with the bulk electrodes and using localized basis sets,

DOI: 10.1021/acs.jpcc.5b03635
J. Phys. Chem. C XXXX, XXX, XXX−XXX

the NEGF for the scattering region $\mathcal{G}(E, V)$ can be formulated as following:

$$\mathcal{G}(E, V) = [E \times S_S - H_S[\rho] - \Sigma_L(E, V) - \Sigma_R(E, V)]^{-1} \quad (2)$$

where S_S and H_S are the overlap matrix and the Hamiltonian, respectively, for the scattering region. $\Sigma_{L/R}$ are self-energies that account for the effect from the left (L) and right (R) electrodes upon the central region. The self-energies are given by $\Sigma_\alpha = V_{S\alpha} g_\alpha V_{\alpha S}$, where g_α are the surface Green's functions for the semi-infinite leads and $V_{\alpha S} = V_{S\alpha}^\dagger$ are the coupling matrix elements between the electrodes and the scattering region. The Hamiltonians can be calculated through several approaches (e.g., using tight-binding methods). Actually, H_S is a functional of electronic density and for this reason, we used the Hamiltonian obtained from the DFT calculations. The charge density is self-consistently calculated via Green's functions until convergence is achieved; the transmission coefficient $T(E)$ can be obtained as

$$T(E) = \Gamma_L(E, V)\mathcal{G}(E, V)\Gamma_R(E, V)\mathcal{G}^\dagger(E, V) \quad (3)$$

where the coupling matrices are given by $\Gamma_\alpha = i[\Sigma_\alpha - \Sigma_\alpha^\dagger]$, with $\alpha \equiv \{L, R\}$. Further details regarding the methods for calculating electronic transport properties can be found in the literature.[45,46]

RESULTS AND DISCUSSION

Adsorption Configurations. Figure 1 (left panel) shows a schematic device setup for P- and (B and N) doped-silicene used for gas detection. First, we address the structural stability of molecular adsorption geometries by initially placing each molecule on P- and B/N- silicene, respectively. For P-silicene, there are at least four possible starting adsorption sites: hill, valley, hollow and bridge sites. For doped sensors (B and N), only the gas adsorption above the B and N atoms and their nearest neighbors were tested. For these positions, different molecular orientations were examined. For diatomic gases (CO and NO), we investigated three possible orientations. Their molecular axis was oriented parallel and perpendicular (with the O pointing up and down) with respect to the silicene surface. For tri- and tetratomic gases (NO_2 and NH_3), two orientations were tested, i.e., one with the N atom pointing to the surface and the other with the N atom pointing away from the surface. The most stable adsorption configurations of each molecular gas on the silicene devices are presented in Figure 1 (central and right panels). A more detailed discussion of other less stable adsorption configurations can be found in the Supporting Information. For P-silicene, in principle, there is no favorable site to adsorb the molecular gas. The interaction of NH_3 and CO with P-silicene is mostly of van der Waals type, whereas NO and NO_2 exhibit covalent chemisorption bonding. For doped devices, the gas molecules energetically prefer to be chemisorbed on the top of a B atom for B-silicene and chemisorbed on the top of a Si atom nearest to the N dopant for N-silicene. The binding energies of doped-silicene become larger than that of pristine, and the binding distances between the gases and doped-devices are shortened (see Table 1) as expected.

To better understand the binding strength of gas adsorption, we analyzed the charge density of three nanosensors, i.e., pristine and with the two dopants, as shown in Figure 2. The

Table 1. Calculated Binding Energy (E_b), Binding Distance (D),[a] and Charge Transfer from the Silicene to Molecules $\Delta Q(|e|)$

devices	gas	E_b (eV)	D (Å)	$\Delta Q(\lvert e\rvert)$
P-silicene	NO	−0.73	2.11	0.19
	NO_2	−1.30	1.77	0.37
	NH_3	−0.26	2.27	0.16
	CO	−0.10	3.24	−0.03
B-silicene	NO	−1.01	1.46	0.19
	NO_2	−3.02	1.50	0.08
	NH_3	−0.80	1.63	0.49
	CO	−1.19	1.51	0.32
N-silicene	NO	−1.95	1.87	0.01
	NO_2	−3.50	1.76	−0.06
	NH_3	−0.80	2.06	0.42
	CO	−0.99	1.88	0.20

[a]Binding distance (D) is defined as the shortest atom-to-atom distance between the molecule and silicene.

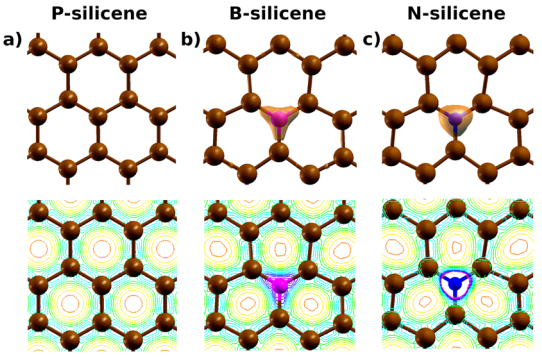

Figure 2. Charge density for (a) pristine silicene; (b) B-doped silicene, and (c) N-doped silicene. The plotted isosurface corresponds to a value of 0.08 $e \times \text{bohr}^{-3}$ for all panels.

pristine device was considered a neutral device, in which the charge density is equally distributed through the device. Although the doped nanodevices were also neutral, they had charge localization in the vicinity of each dopant that led to the conclusion that atoms had electron acceptor and donor characteristics for B and N dopants, respectively. We furthermore considered the electronegativity of all species involved in the devices. For B-silicene, the charge is concentrated close to B (it became slightly negative) and the three nearest-neighbor Si partially share this charge. The second device doped with N has higher charge accumulation close to N, compared to the former case, and the neighbor Si atoms become less charged. These facts are due to the electronegativity hierarchy of Si and dopant atoms; (N ≫ B ≳ Si). N has a tendency to attract electrons more strongly than B and Si. Figure 2 confirms this assumption that the charge was localized on the dopant for N-silicene and spread up the bonds for the B-silicene system.

The binding sites and molecular orientations of adsorbed gases on the nanosensor devices (Figure 1) needs to be discussed in more detail. For example, NO with an odd number of valence electrons has one unpaired electron on N atom which makes it highly reactive. As a result, NO always binds to the pristine silicene with N atom (see panel NO in center of Figure 1). As the second case in point, NH_3 has a tendency to bind to the pristine system with N, while the three H atoms

DOI: 10.1021/acs.jpcc.5b03635
J. Phys. Chem. C XXXX, XXX, XXX−XXX

point up. This is the simplest case because NH_3 has a lone pair on a N atom. The interesting case is for N-silicene, both dopant and gas have N atoms with the same electronegativity. Consequently, the NH_3 prefer binding with one Si atom close to a N atom (see Figure 1). Comparing the adsorption of NH_3, NO, and NO_2 on P-silicene with previously reported results,[36] our calculated binding energies are seen to differ in general by less than approximately 18%, however, the disagreement is larger for NH_3. When compared to the binding energy and the charge transfer of NH_3 on P-silicene in ref 15, our results agree quite well; there is a difference of 28.8% for binding energy and the value of charge transfer is exactly the same. The variation in results could be due to the difference of localized basis and plane-wave basis as well as the difference of dispersion correction. Additionally, our results are found to be in good agreement with a previous DFT study[35] except for the cases of physisorbed gases, i.e., CO and NH_3. The binding energy difference between those results and ours for NH_3 amounts to almost 60%. This large discrepancy stems from the inclusion of the long-range van der Waals (vdW) interactions in our present work. Furthermore, we systematically optimized the adsorption geometry of each gas molecule considering various possible molecular orientations and adsorption sites as a starting point for each relaxation (see the Supporting Information). Overall, we find qualitatively good agreement with previous studies for the most stable configuration of the adsorbate on P-silicene. However, when the device is doped, the gas prefers binding to the devices with a C atom. Finally, for NO_2 on P- and N-silicene devices, a covalent bond is formed between the Si atom and O atom due to the existence of an unpaired electron on one of the O atoms. For B-silicene, it is more energetically favorable that NO_2 binds to the system with its N atom. This results from the coordinate covalent bond in which an electron pair on the N atom enter into a vacant p-orbital on the B atom.

Possibility of Silicene Device as a Gas Sensor. Two of the most important challenges to build a good commercial sensor are the ability to detect different harmful gases (selectivity) and to improve the ability to sense some gas molecules (sensitivity). Experimentally, one of the most important parameters for sensing a gas is usually a variation in resistance or conductance, known as sensitivity. This property can be defined as $S\ (\%) = \frac{|G - G_0|}{G_0}$, where G and G_0 are the zero bias conductance for nanosensor with and without gas, respectively. Here, the conductance was simply calculated as $G = G_0 T(E_F)$, where $G_0 = 2e^2/h$ is the quantum conductance, e is the charge of the electron and h is Planck's constant.

The transmittance $T(E)$ of the P-, B-, and N-silicene devices is presented in Figure 3, parts a–c, respectively. Obviously, the gas adsorption significantly affects the $T(E)$ of the three devices. For example, the adsorption of NO and NO_2 on P-silicene results in a remarkable decrease of the $T(E)$, whereas for CO and NH_3 the changes are not very pronounced. Additionally, the results indicate that doping either B or N atoms into silicene improves the detection of CO and NH_3, compared to that of P-silicene. Without the presence of gas, the $T(E)$ of doped-silicene was lower than that of the P-silicene (as depicted by the black dashed line in Figure 3). The $T(E)$ of B-silicene was lower than that of N-silicene. It was shown that the

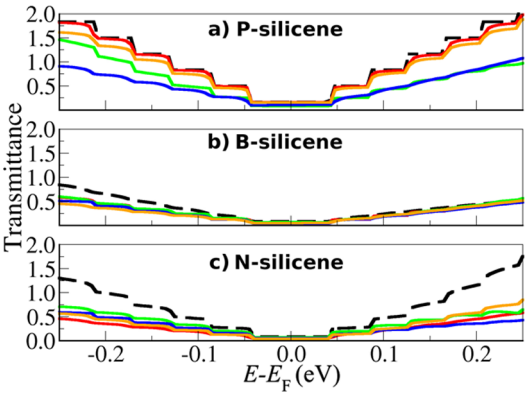

Figure 3. Transmittance as a function of energy E, where the Fermi energy (E_F) is set at zero, is shown for (a) P-silicene; (b) B-silicene, and (c) N-silicene. Red, green, orange, and blue lines represent the transmittance for CO, NO, NH_3, and NO_2 adsorbed on the devices, respectively, while black dashed lines represent that of the reference system (P-, B-, and N-silicene devices without gas).

gas adsorption on the B-silicene device affected the $T(E)$, but not as strongly as for N-silicene.

Figure 4a presents the sensitivity as a function of binding energy of the three devices (P-, B-, and N-silicene) for NO, NO_2, NH_3, and CO gas molecules. In order to evaluate whether silicene and doped silicene can be good gas nanosensors, we should have both high and distinct sensitivities when the sensor is exposed to different gases. Another important aspect is about how long the gas can stay on the device. This is the residence time (τ) and it is proportional to $\approx \exp\left(\frac{-E_b}{k_B T}\right)$, where E_b is binding energy, k_B is the Boltzmann constant and T is temperature. We expect small binding energies to lead to fast desorption of gases from the devices. Analyzing Figure 4a, we found that the binding energies were generally less than 2 eV. The only exception occurred for NO_2 on the doped-devices ($E_b > 3$ eV). Turning our focus to each device, we observed that the P-silicene device (see Figure 4b) has binding energies ranging from −0.1 to −1.3 eV and their respective sensitivities were strongly dependent on gas molecules. The sensitivity of the P-silicene device increased linearly with increasing binding energy. The sensitivities were found to follow an ascending order; i.e., CO < NH_3 < NO < NO_2. However, CO and NH_3 have low sensitivity. Spin-polarized calculations were also performed, but the resulting energy differences are smaller than the thermal fluctuations at the envisioned operating temperature of the sensor, namely room temperature ($k_B T \approx 0.025$ eV). In a test, we found that the transmittance for each channel (up and down) exhibits only minor quantitative differences which do not affect our conclusions. For these reasons, spin polarization effects were neglected in our study.

Next, we will address how to improve the sensitivity of these gases. As can be seen in Figure 4a, by the introduction of dopant atoms, N-silicene (diamond shape) and B-silicene (square shape) exhibited higher binding energies and subsequently sensitivity. This is especially true for CO and NH_3 (see Figure 4, parts c and d). Better sensitivity was obtained due to increased binding energies (see Table 1). Interestingly, CO molecules can distinguish p-type and n-type doping of silicene (see Figure 4c). This contradicts the findings of a previous study of a graphene-based gas sensor.[7] The CO on N-doped silicene showed a sensitivity around 2 orders of

DOI: 10.1021/acs.jpcc.5b03635
J. Phys. Chem. C XXXX, XXX, XXX−XXX

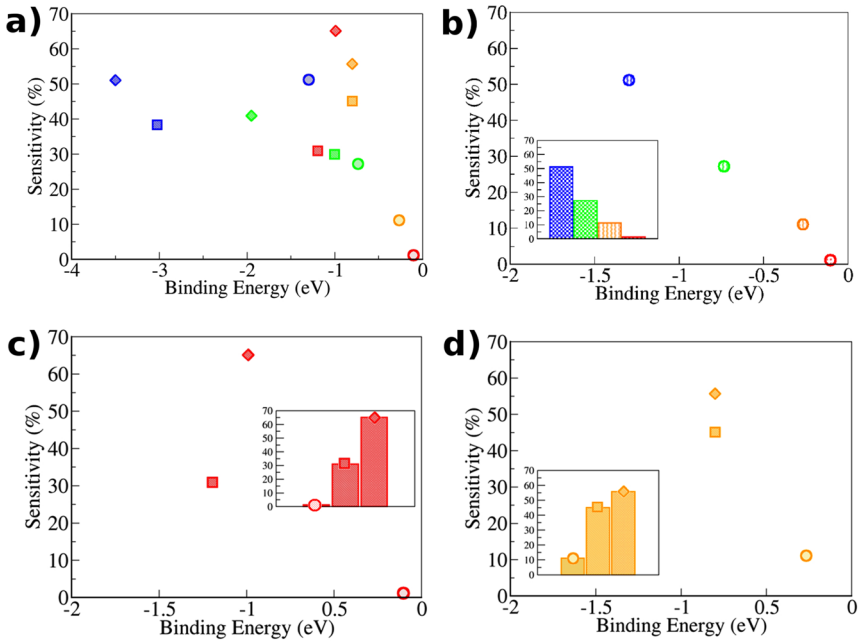

Figure 4. (a) Sensitivity versus binding energy for NO (green), NO_2 (blue), NH_3 (orange) and CO (red) gas molecules on P-silicene (circle), B-silicene (square) and N-silicene (diamond) devices, respectively; (b) the four gas species on P-siliene (the inset shows the sensitivity comparison for P-silicene); (c) CO on three devices and (d) NH_3 on three devices. The insets of parts c and d are the sensitivity comparison for one gas on the three different devices.

magnitude higher than that of CO on B-doped silicene. To explain why the sensitivity increased substantially for these molecular gases, the charge transfer of these systems will be investigated.

The transport properties of silicene devices relate to the change in local charge distribution around the B and N impurity atoms as a consequence of the charge transfer from gas molecules adsorbed on silicene. To visualize the charge transfer of NH_3 and CO adsorbed on the devices, we calculate the charge density difference $\Delta\rho(\vec{r}) = \rho_{device+gas}(\vec{r}) - (\rho_{device}(\vec{r}) + \rho_{gas}(\vec{r}))$, as presented in Figure 5.

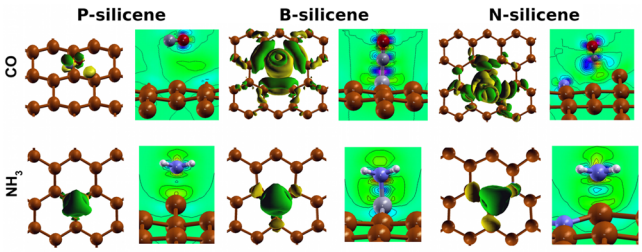

Figure 5. Charge density difference for CO (upper) and NH_3 (lower panel) on P-, B-, and N-silicene devices for each type of nanosensor. Isosurfaces are plotted for isovalues of 0.0004 (0.002) $e \times \text{bohr}^{-3}$ for CO (NH_3) alongside contour plots. For the isosurface plots, green color represents negative charge density difference while yellow corresponds to a positive change in charge density.

The contour plot of $\Delta\rho$ illustrates the charge accumulation/depletion in the system, i.e., we can quantitatively describe the idea of the charge transfer. For doped silicene, there is charge accumulation indicating the hybridization of orbitals at the nanosensor surface in which NH_3 and CO is adsorbed (see Figure 5). Such orbital hybridization is absent for physisorption of the gases on P-silicene. In other words, the charge-transfer capability increases with the increasing bonding charge densities.

Furthermore, we investigated the electron charge transfer using the Mulliken population analysis (see Table 1). It is notable that the positive charge transfer occurred from the gas molecules to the silicene. As discussed above, our results reveal the difference in charge redistribution of three nanosensors (see Figure 2). For B-silicene, as shown in Table 1, all gases examined in the current study act as donors. They donate charges to the device, resulting from the vacant p-orbital on the B atom. A large amount of charge transfer is obtained, especially for NH_3, which is electron-donating molecule. For N-silicene, the electron-rich gas molecules prefer to adsorb on the top of one positively charged Si close to N (see Figure 1). A negative charge transfer value as observed only for NO_2 due to its strong electron-withdrawing capabilities.

A few important aspects should also be discussed. The first is the influence of substrates on gas sensing performance. According to the experimental studies, for all the cases, silicene was synthesized on top of some substrates.[20−22,24] A very recent study[35] elaborated the effect of Ag(111) substrate on the electronic structures of gas molecules on silicene, indicating a slight increase in adsorption energies and charge transfer. We expected that the conductance could be changed due to the influence of different substrates, changing the sensitivity, but the interaction between silicene should not substantially change the overall trend with this additional component. The second point is about the experimental challenge to control the doping in silicene. Recent experimental studies reported on potassium adsorption in silicene,[47] inducing n-type doping. Additionally, a theoretical study also showed the stability of B/N substituted doping into silicene.[48] Therefore, if reactive centers can be created as we have shown, their gas sensing performance will be improved enormously. In addition, there remain many challenging problems. For instance, a recent study[49] demonstrated the dissociative adsorption of molecules (H_2, O_2, CO,

DOI: 10.1021/acs.jpcc.5b03635
J. Phys. Chem. C XXXX, XXX, XXX−XXX

H_2O, and OH) on defect sites in graphene and silicene. In our study, these molecules remain intact on silicene, but certain molecules may dissociate due to increased chemical reactivity at the defect sites as it has been reported previously.[49]

CONCLUSIONS

In conclusion, we investigated the capability of silicene-based devices for sensing chemical gases in terms of sensitivity and selectivity. We employed first-principles electronic structure calculations based on density functional theory formalism. For adsorption of NO, NO_2, NH_3, and CO on pristine (P-), B-doped, or N-doped silicene, we determine the adsorption configurations, binding energies, charge transfer and change in the electronic transport properties. Our results reveal that P-silicene can detect NO and NO_2 gas molecules with high sensitivity. However, this is limited to CO and NH_3 due to weak van der Waals interaction between those gases and P-silicene. By doping P-silicene with either B or N atoms, enhanced binding and charge transfer of all studied gases on the nanosensor were achieved, resulting in an increased sensitivity toward NH_3 and CO detection. However, doped-silicene strongly bound to NO and NO_2 is not presumably suitable for practical gas sensor devices. On the basis of our results, we can conclude that by doping with different impurities, one can create a silicene device that is able to detect different gas species with high sensitively and selectivity.

ASSOCIATED CONTENT

Supporting Information

Starting configurations for P-silicene and B/N-doped silicene. The Supporting Information is available free of charge on the ACS Publications website at DOI: 10.1021/acs.jpcc.5b03635.

AUTHOR INFORMATION

Corresponding Author

*(J.P.) E-mail: jariyanee.prasongkit@npu.ac.th. Telephone: +66 42 587 306 Fax: +66 42 587 306.

Present Address

[⊥]Departamento de Química, Instituto Tecnológico de Aeronáutica, São José dos Campos, São Paulo, Brazil.

Notes

The authors declare no competing financial interest.

ACKNOWLEDGMENTS

J.P. gratefully acknowledges financial support from the Thailand Research Fund (MRG5680186). R.G.A. and S.C were both supported by scholarships from the Carl Tryggers Foundation. R.H.S. would like to thank the Swedish Research Council (VR, Grant No. 621-2009-3628) for financing his position, and the Gender Equality Fund from the Department of Physics and Astronomy at Uppsala University for inviting J.P. for a research visit there. R.A. would also like to acknowledge the Swedish Research Council (VR, Grant No. 621-2012-4379) and Swedish Energy Agency. V.A. would like to thank the Nanotechnology Center (NANOTEC), NSTDA, Ministry of Science and Technology, Thailand, through its program of Centers of Excellence Network. The Swedish National Infrastructure for Computing (SNIC), the Uppsala Multidisciplinary Center for Advanced Computational Science (UPPMAX), and Versatus HPC provided computing time for this project.

REFERENCES

(1) Schedin, F.; Geim, A. K.; Morozov, S. V.; Hill, E. W.; Blake, P.; Katsnelson, M. I.; Novoselov, K. S. Detection of Individual Gas Molecules Adsorbed on Graphene. *Nat. Mater.* **2007**, *6*, 652−655.

(2) He, Q.; Wu, S.; Yin, Z.; Zhang, H. Graphene -Based Electronic Sensors. *Chem. Sci.* **2012**, *3*, 1764−1772.

(3) Fowler, J. D.; Allen, M. J.; Tung, V. C.; Yang, Y.; Kaner, R. B.; Weiller, B. H. Practical Chemical Sensors from Chemically Derived Graphene. *ACS Nano* **2009**, *3*, 301−306.

(4) Some, S.; Xu, Y.; Kim, Y.; Yoon, Y.; Qin, H.; Kulkarni, A.; Kim, T.; Lee, H. Highly Sensitive and Selective Gas Sensor Using Hydrophilic and Hydrophobic Graphenes. *Sci. Rep.* **2013**, *3*, 1868.

(5) Deng, S.; Tjoa, V.; Fan, H. M.; Tan, H. R.; Sayle, D. C.; Olivo, M.; Mhaisalkar, S.; Wei, J.; Sow, C. H. Reduced Graphene Oxide Conjugated Cu_2O Nanowire Mesocrystals for High-Performance NO_2 Gas Sensor. *J. Am. Chem. Soc.* **2012**, *134*, 4905−4917.

(6) Leenaerts, O.; Partoens, B.; Peeters, F. Adsorption of H_2O, NH_3, CO, NO_2, and NO on Graphene: A First-Principles Study. *Phys. Rev. B: Condens. Matter Mater. Phys.* **2008**, *77*, 125416.

(7) Zhang, Y.-H.; Chen, Y.-B.; Zhou, K.-G.; Liu, C.-H.; Zeng, J.; Zhang, H.-L.; Peng, Y. Improving Gas Sensing Properties of Graphene by Introducing Dopants and Defects: A First-Principles Study. *Nanotechnology* **2009**, *20*, 185504.

(8) Dai, J.; Yuan, J.; Giannozzi, P. Gas Adsorption on Graphene Doped with B, N, Al, and S: A Theoretical Study. *Appl. Phys. Lett.* **2009**, *95*, 232105.

(9) Cahangirov, S.; Topsakal, M.; Aktürk, E.; Şahin, H.; Ciraci, S. Two- and One-Dimensional Honeycomb Structures of Silicon and Germanium. *Phys. Rev. Lett.* **2009**, *102*, 236804.

(10) Jose, D.; Datta, A. Structures and Chemical Properties of Silicene: Unlike Graphene. *Acc. Chem. Res.* **2014**, *47*, 593−602.

(11) Lin, X.; Ni, J. Much Stronger Binding of Metal Adatoms to Silicene than to Graphene: A First-Principles Study. *Phys. Rev. B: Condens. Matter Mater. Phys.* **2012**, *86*, 075440.

(12) Vogt, P.; De Padova, P.; Quaresima, C.; Avila, J.; Frantzeskakis, E.; Asensio, M. C.; Resta, A.; Ealet, B.; Le Lay, G. Silicene: Compelling Experimental Evidence for Graphenelike Two-Dimensional Silicon. *Phys. Rev. Lett.* **2012**, *108*, 155501.

(13) Houssa, M.; van den Broek, B.; Scalise, E.; Pourtois, G.; Afanas'ev, V. V.; Stesmans, A. An electric field tunable energy band gap at silicene/(0001) ZnS interfaces. *Phys. Chem. Chem. Phys.* **2013**, *15*, 3702−3705.

(14) Drummond, N. D.; Zólyomi, V.; Fal'ko, V. I. Electrically Tunable Band Gap in Silicene. *Phys. Rev. B: Condens. Matter Mater. Phys.* **2012**, *85*, 075423.

(15) Kaloni, T. P.; Schreckenbach, G.; Freund, M. S. Large Enhancement and Tunable Band Gap in Silicene by Small Organic Molecule Adsorption. *J. Phys. Chem. C* **2014**, *118*, 23361−23367.

(16) Denis, P. A. Stacked Functionalized Silicene: A Powerful System to Adjust the Electronic Structure of Silicene. *Phys. Chem. Chem. Phys.* **2015**, *17*, 5393−5402.

(17) Kaloni, T. P.; Singh, N.; Schwingenschlögl, U. Prediction of a Quantum Anomalous Hall State in Co-Decorated Silicene. *Phys. Rev. B: Condens. Matter Mater. Phys.* **2014**, *89*, 035409.

(18) Houssa, M.; Pourtois, G.; Heyns, M. M.; Afanas'ev, V. V.; Stesmans, A. Electronic Properties of Silicene: Insights from First-Principles Modelling. *ECS Trans.* **2010**, *33*, 185−193.

(19) Lazar, P.; Karlický, F.; Jurečka, P.; Kocman, M.; Otyepková, E.; Šafářová, K.; Otyepka, M. *J. Am. Chem. Soc.* **2013**, *135*, 6372−6377.

(20) Feng, B.; Ding, Z.; Meng, S.; Yao, Y.; He, X.; Cheng, P.; Chen, L.; Wu, K. Evidence of Silicene in Honeycomb Structures of Silicon on Ag(111). *Nano Lett.* **2012**, *12*, 3507−3511.

(21) Vogt, P.; De Padova, P.; Quaresima, C.; Avila, J.; Frantzeskakis, E.; Asensio, M. C.; Resta, A.; Ealet, B.; Le Lay, G. Silicene: Compelling Experimental Evidence for Graphenelike Two-Dimensional Silicon. *Phys. Rev. Lett.* **2012**, *108*, 155501.

(22) Rachid Tchalala, M.; Enriquez, H.; Mayne, A. J.; Kara, A.; Roth, S.; Silly, M. G.; Bendounan, A.; Sirotti, F.; Greber, T.; Aufray, B.; et al.

DOI: 10.1021/acs.jpcc.5b03635
J. Phys. Chem. C XXXX, XXX, XXX−XXX

Formation of One-Dimensional Self-Assembled Silicon Nanoribbons on Au(110)-(21). *Appl. Phys. Lett.* **2013**, *102*, 083107.
(23) Fleurence, A.; Friedlein, R.; Ozaki, T.; Kawai, H.; Wang, Y.; Yamada-Takamura, Y. Experimental Evidence for Epitaxial Silicene on Diboride Thin Films. *Phys. Rev. Lett.* **2012**, *108*, 245501.
(24) Meng, L.; Wang, Y.; Zhang, L.; Du, S.; Wu, R.; Li, L.; Zhang, Y.; Li, G.; Zhou, H.; Hofer, W. A.; et al. Buckled Silicene Formation on Ir(111). *Nano Lett.* **2013**, *13*, 685−690.
(25) Tsai, W.-F.; Huang, C.-Y.; Chang, T.-R.; Lin, H.; Jeng, H.-T.; Bansil, A. Gated silicene as a tunable source of nearly 100% spin-polarized electrons. *Nat. Commun.* **2013**, *4*, 1500.
(26) Xu, C.; Luo, G.; Liu, Q.; Zheng, J.; Zhang, Z.; Nagase, S.; Gao, Z.; Lu, J. Giant Magnetoresistance in Silicene Nanoribbons. *Nanoscale* **2012**, *4*, 3111−3117.
(27) Ni, Z.; Zhong, H.; Jiang, X.; Quhe, R.; Luo, G.; Wang, Y.; Ye, M.; Yang, J.; Shi, J.; Lu, J. Tunable Band Gap and Doping Type in Silicene by Surface Adsorption: Towards Tunneling Transistors. *Nanoscale* **2014**, *6*, 7609−7618.
(28) Liu, H.; Gao, J.; Zhao, J. Silicene on Substrates: A Way to Preserve or Tune Its Electronic Properties. *J. Phys. Chem. C* **2013**, *117*, 10353−10359.
(29) Ni, Z.; Liu, Q.; Tang, K.; Zheng, J.; Zhou, J.; Qin, R.; Gao, Z.; Yu, D.; Lu, J. Tunable Bandgap in Silicene and Germanene. *Nano Lett.* **2012**, *12*, 113−118.
(30) Tao, L.; Cinquanta, E.; Chiappe, D.; Grazianetti, C.; Fanciulli, M.; Dubey, M.; Molle, A.; Akinwande, D. Silicene Field-Effect Transistors Operating at Room Temperature. *Nat. Nanotechnol.* **2015**, *10*, 227−231.
(31) Jose, D.; Datta, A. Structures and Electronic Properties of Silicene Clusters: A Promising Material for FET and Hydrogen Storage. *Phys. Chem. Chem. Phys.* **2011**, *13*, 7304−7311.
(32) Hussain, T.; Chakraborty, S.; Ahuja, R. Metal-Functionalized Silicene for Efficient Hydrogen Storage. *ChemPhysChem* **2013**, *14*, 3463−3466.
(33) Sadeghi, H.; Bailey, S.; Lambert, C. J. Silicene-Based DNA Nucleobase Sensing. *Appl. Phys. Lett.* **2014**, *104*, 103104.
(34) Amorim, R. G.; Scheicher, R. H. Silicene as a New Potential DNA Sequencing Device. *Nanotechnology* **2015**, *26*, 154002.
(35) Feng, J.-w.; Liu, Y.-j.; Wang, H.-x.; Cai, Q.-h.; Wang, X.-z. Gas Adsorption on Silicene: A Theoretical Study. *Comput. Mater. Sci.* **2014**, *87*, 218−226.
(36) Hu, W.; Xia, N.; Wu, X.; Li, Z.; Yang, J. Silicene as a Highly Sensitive Molecule Sensor for NH_3, NO and NO_2. *Phys. Chem. Chem. Phys.* **2014**, *16*, 6957−6962.
(37) Hohenberg, P.; Kohn, W. Inhomogeneous Electron Gas. *Phys. Rev.* **1964**, *155*, 864−870.
(38) Kohn, W.; Sham, L. Self-Consistent Equations Including Exchange and Correlation Effects. *Phys. Rev.* **1965**, *385*, 1133−1138.
(39) Soler, M.; Artacho, E.; Gale, J. D.; Garcia, A.; Junquera, J.; Ordejon, P.; Sánchez-Portal, D. The SIESTA Method for Ab Initio Order- N Materials. *J. Phys.: Condens. Matter* **2002**, *14*, 2745−2779.
(40) Dion, M.; Rydberg, H.; Schröder, E.; Langreth, D. C.; Lundqvist, B. I. Van der Waals Density Functional for General Geometries. *Phys. Rev. Lett.* **2004**, *92*, 246401.
(41) Román-Pérez, G.; Soler, J. Efficient Implementation of a van der Waals Density Functional: Application to Double-Wall Carbon Nanotubes. *Phys. Rev. Lett.* **2009**, *103*, 096102.
(42) Perdew, J. P.; Burke, K.; Ernzerhof, M. Generalized Gradient Approximation Made Simple. *Phys. Rev. Lett.* **1996**, *77*, 3865−3868.
(43) Troullier, N. Efficient Pseudopotentials for Plane-Wave Calculations. *Phys. Rev. B: Condens. Matter Mater. Phys.* **1991**, *43*, 1993−2006.
(44) Kresse, G.; Furthmüller, J. Efficient Iterative Schemes for Ab Initio Total-Energy Calculations Using a Plane-Wave Basis Set. *Phys. Rev. B: Condens. Matter Mater. Phys.* **1996**, *54*, 11169.
(45) Brandbyge, M.; Mozos, J.-L.; Ordejón, P.; Taylor, J.; Stokbro, K. Density-Functional Method for Nonequilibrium Electron Transport. *Phys. Rev. B: Condens. Matter Mater. Phys.* **2002**, *65*, 165401.
(46) Rocha, A.; García-Suárez, V.; Bailey, S.; Lambert, C.; Ferrer, J.; Sanvito, S. Spin and Molecular Electronics in Atomically Generated Orbital Landscapes. *Phys. Rev. B: Condens. Matter Mater. Phys.* **2006**, *73*, 085414.
(47) Friedlein, R.; Fleurence, A.; Sadowski, J. T.; Yamada-Takamura, Y. Tuning of Silicene-Substrate Interactions with Potassium Adsorption. *Appl. Phys. Lett.* **2013**, *102*, 221603.
(48) Sivek, J.; Şahin, H.; Partoens, B.; Peeters, F. M. Adsorption and Absorption of Boron, Nitrogen, Aluminum, and Phosphorus on Silicene: Stability and Electronic and Phonon Properties. *Phys. Rev. B: Condens. Matter Mater. Phys.* **2013**, *87*, 085444.
(49) Gürel, H. H.; Özçelik, V. O.; Ciraci, S. Dissociative Adsorption of Molecules on Graphene and Silicene. *J. Phys. Chem. C* **2014**, *118*, 27574−27582.

DOI: 10.1021/acs.jpcc.5b03635
J. Phys. Chem. C XXXX, XXX, XXX−XXX

Supplementary Material for: Highly sensitive and selective gas detection based on silicene

Jariyanee Prasongkit,[*,†,‡] Rodrigo G. Amorim,[¶] Sudip Chakraborty,[¶] Rajeev Ahuja,[¶,§] Ralph H. Scheicher,[¶] and Vittaya Amornkitbamrung[‖,‡]

Division of Physics, Faculty of Science, Nakhon Phanom University, Nakhon Phanom, 48000, Thailand, Nanotec-KKU Center of Excellence on Advanced Nanomaterials for Energy Production and Storage, Khon Kaen 40002, Thailand., Division of Materials Theory, Department of Physics and Astronomy, Box 516, Uppsala University, SE-751 20 Uppsala, Sweden, Applied Materials Physics, Department of Materials Science and Engineering, Royal Institute of Technology (KTH), SE-100 44 Stockholm, Sweden, and Department of Physics, Faculty of Science, Khon Kaen University, 123 Mittraphab Road, Khon Kaen 40002, Thailand

E-mail: jariyanee.prasongkit@npu.ac.th

Unit cell and supercell

Silicene has a hexagonal lattice with two atoms per unit cell (A and B) as is shown in Figure S1-a. However, is also possible define an unit cell with four atoms and parallepiped shape (see Figure S1-b), in which the lattice is characterized by three lattice vectors L_x, L_y and L_z. In particular both unit cells are equivalent, but as we are interested in transport properties through the device

[*]To whom correspondence should be addressed
[†]Nakhon Phanom University
[‡]Nanotec-KKU Center of Excellence on Advanced Nanomaterials for Energy Production and Storage
[¶]Uppsala University
[§]Royal Institute of Technology
[‖]Khon Kaen University

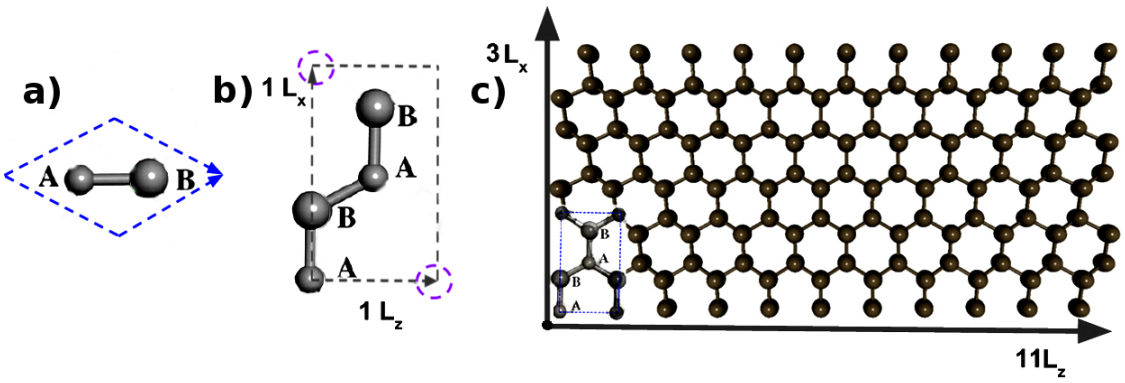

Figure S1: a) Hexagonal 2D lattice with two atoms per unit cell for silicene; b) A parallelepiped unit cell with four atoms per unit cell and (c) supercell used in relaxations and also transport calculation.

in certain direction, the parallelepiped unit cell fits better for this application. In all calculation were employed a supercell using a parellepiped unit cell with $3L_x \times L_y \times 11L_z$ *and 132 atoms as is shown in Figure S1-c. The referred supercell has* $20.57\text{Å} \times 15\text{Å} \times 43.54\text{Å}$.

Geometry relaxation

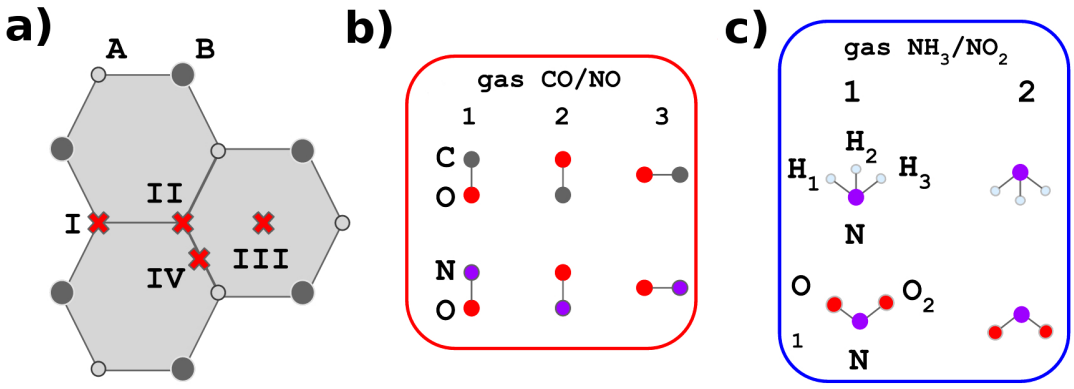

Figure S2: (a) Possible adsorption sites of gases on the hexagonal lattice of P-silicene: (I) hill, (II) valley, (III) bridge, and (IV) hollow sites. Different molecular orientations were examined for (b) CO and NO (diatomic gas molecules) with three possible orientations and (c) NH_3 and NO_2 (tri- and tetra-atomic gas molecules) with two initial orientations.

Figure S2-(a) shows four possible adsorption sites of gases on the P-silicene. They are referred to as the (I) hill, (II) valley, (III) bridge, and (IV) hollow sites. For these positions, different

molecular orientations were examined. For diatomic gases (CO and NO), we investigated three possible orientations. Their molecular axis was oriented parallel and perpendicular (with the O pointing up and down) with respect to the silicene surface. For tri- and tetra- atomic gases (NH_3 and NO_2), two orientations were tested, i.e., one with the N atom pointing to the surface and the other with the N atom pointing away from the surface. These can be seen in Figure S2-(b,c).

For P-silicene, twelve starting configurations for CO and NO (diatomic gases) and eight for NO_2 and NH_3 (tri-/tetra- atomic gases) were considered. Note that the starting configuration was not the final one. We sometimes see energy degenerated structures with very small binding energy differences. CO has two degenerate adsorption configurations, i.e., III-3 and IV-3. NO exhibits two most stable configurations, i.e., II-2 and III-2. NH_3 presents two degenerate adsorption configurations, i.e, IV-1 and II-1. The most stable configurations including its binding energy and binding distance are presented in the main manuscript.

For doped-silicene, we examined only the gas adsorption above the dopants and their nearest neighbors since these adsorption sites are the most active. As shown in the main manuscript, we observed that different gases exhibit distinct configurations for each doped-silicene device. CO and NO (diatomic gases) binding with the doped-silicene at the C and N atom, respectively. They were tilted with respect to the surface for N- silicene, but aligned perpendicularly for B-silicene. NH_3 bonds to the silicene with its N atom for both doped-devices. NO_2 bonds to B-silicene with its N atom (B-N bond) and to N-silicene with an O atom (Si–O bond).